Vibration Analysis for Damage Detection and Classification for Condition Monitoring on Worm Gears

Philipp Häderle[1], Martin Dazer[2], and Patric Schmitt[3]

[1,2] *University of Stuttgart, Institute of Machine Components, Stuttgart, BW, 70569, Germany*
philipp.haederle@ima.uni-stuttgart.de
martin.dazer@ima.uni-stuttgart.de

[3]*AUMA Riester GmbH & Co. KG, Müllheim, BW, 79379, Germany*
patric.schmitt@auma.com

ABSTRACT

Worm gears exhibit a higher proportion of sliding motion during tooth meshing than spur gears. Typically, this type of gear consists of a soft worm wheel, often made of brass, and a hard steel worm. These characteristics promote the occurrence of abrasive wear and further fatigue damage during operation. The objective of this study is the vibration data analysis for a sensor-based detection and classification of two types of damage in worm gears during operation. For this purpose, a data set is available containing the measurement data from an accelerometer under various operating conditions with regard to rotational speed and torque. The data set comprises measurements of the undamaged condition, artificial tooth thickness reduction on the worm wheel to reflect wear, and artificial breakouts reflecting pitting damage on the worm. For damage detection the accelerometer data is evaluated in the frequency domain. The amplitudes at different frequencies are analyzed for each type of damage. Both types of damage exhibit distinct characteristics in the analyzed frequency spectra. Based on these differences, vibration-based indicators are derived from the frequency spectra, enabling the detection and classification of breakout damage on the worm and wear damage on the worm wheel. Breakout damage on the worm is characterized by a discrepancy in the acceleration amplitudes at the harmonics of the gear mesh frequency when compared to measurements obtained under undamaged conditions. For the wear damage on the worm wheel, a systematic difference compared to the undamaged reference measurement can be detected in the frequency range between 7.5 kHz and 8.5 kHz. In addition to the effect of the damage, a distinct influence of the rotational speed and torque is observed on the extracted indicators for damage detection. Since different data evaluation methods are best suited for detecting each type of damage, damage classification is possible. In the context of PHM, this enables health management measures to be implemented according to the severity of the detected type of damage.

1. INTRODUCTION

Worm gears are utilized in applications where high transmission ratios and smooth operation are required. In most worm gears, a hard steel worm and a softer material worm wheel are employed to optimize tribological conditions. Since most worm gears do not feature involute tooth shapes, this material pairing facilitates the development a contact pattern trough initial wear on the soft worm wheel during the run-in process. This initial wear on the worm wheel is known to decrease after the run-in process, but does not cease completely (Daubach, Oehler & Sauer, 2022; Sharif, Evans & Snidle, 2006). In safety-related applications of worm gears, for instance, in actuators used in power plant technology, continuously progressing damage poses a challenge. In such applications, functionality must be ensured at all times, for example for opening a cooling water pipe. Condition monitoring of the worm gear is therefore essential for maintaining operational safety. If the type of damage can be assessed, health management measures such as condition-based maintenance can be taken.

2. STATE OF THE ART

A multitude of gear damages in worm gears is reported in literature. Also, various approaches for damage detection are presented. The following sections provide a comprehensive overview of known damage types and existing approaches to damage detection.

2.1. Damage Mechanisms in Worm Gears

Pitting, wear, and tooth fracture are the most prevalent types of damage in worm gears (Opalić, Žeželj & Vučković, 2015).

Tao, Chen, Zhang and Jiang (2021) showed that initial cracks at the tooth root of the softer worm wheel, caused by high stress at the beginning of tooth meshing, leads to tooth fracture. The research conducted by Ya-xiong, Ke-jian, Yan, Lin, Zhan-xiu and Wei-min (1988) provides insights into the origin of wear damage in a softer material worm wheel. Microcracks were observed to develop, propagate and merge until small wear particles were abraded from the tooth surface of the worm wheel. Numerous studies have focused on the calculation of wear on the worm wheel (Sharif et al., 2006; Schnetzer, Pellkofer & Stahl, 2023; Jbily, Guingand & Vaujany, 2016). Sharif et al. (2006) calculated wear based on full elastohydrodynamic lubrication in the worm gear. In the studies conducted by Schnetzer et al. (2023), a calculation method for the wear of a bronze worm wheel was derived from experiments conducted on a two-disk test rig. Jibly et al. (2016) applied the Archard wear formula to predict the worm wheel wear as a function of lubrication, contact pressure and bending deflections.

2.2. Damage Detection in Worm Gears

According to Randall (2011), the vibration behavior of machine components is indicative of their health condition. Fundamental investigations on the vibration behavior of worm gears have been conducted by Hammami, Chakroun, Chaari, Hammami, De-Juan, Fernandez, Viadero and Haddar (2022) and Vojtko, Kočiško, Šmeringaiová and Adamčík (2013). The research of Vojtko et al. (2013) suggests a strong correlation between measured vibration amplitudes and the position of the vibration sensor. In addition, a damping effect on the vibration caused by the softer worm wheel is observed by Hammami et al. (2022). The existing literature on damage detection in vibration signals of worm gears is reviewed below.

2.2.1. Detection of Pitting Damage on Worm Wheel

Investigations using artificial pitting damage on the worm wheel have been conducted by Ümütlü, Hizarci, Öztürk and Kiral (2016) and Ümütlü et al. (2020). A variety of time-domain features, including standard deviation, mean, root mean square, peak-to-peak, crest factor, skewness, and kurtosis as well as frequency-domain features such as mean, root mean square, standard deviation, and kurtosis were integrated into an artificial neural network. This neural network was then utilized for the detection and classification of two stages of artificial pitting damage. In the study by Hizarci, Ümütlü, Kiral and Öztürk (2021), the effects of artificial pitting damage on the worm wheel were also examined. Reasoning with the sliding motion during tooth meshing in worm gears, time-domain features were found to be unfeasible for damage detection. Instead, Poincaré plots in combination with a decision tree were applied for condition monitoring. Elasha, Ruiz-Cárcel, Mba, Kiat, Nze and Yebra (2014) evaluated the vibration data of two worm gearboxes, one in an undamaged condition and one with natural pitting damage on the worm wheel. In their study Elasha et al. (2014) demonstrate that the FM4 value was most effective for detecting the pitting damage. Best results were obtained when the vibration data was measured parallel to the shaft of the damaged worm wheel.

2.2.2. Detection of Wear Damage on the Worm Wheel

The most intuitive approach for measuring wear on the worm wheel is to measure the backlash of the worm gear (Sharif et al., 2006; Jibly et al., 2016). However, this approach requires high-resolution encoders, which are not economically viable for condition monitoring in most worm gear applications. Raadnui (2021) investigated the effects of moisture corrosion wear, acid-attacked corrosion wear and three-body abrasive wear in worm gearboxes. In this study, weight measurement and optical surface pattern analysis were applied to detect the different wear modes. In the work of Peng and Kessissoglou (2003) the correlation between vibration signals and wear debris in worm gears was investigated. It was found that the combination of the advantages of these two condition monitoring techniques yielded the best results in terms of damage detection. Waqar and Demetgul (2016) applied vibration and acoustic analysis to detect wear damage on the worm wheel. A detection rate of 94.24 % for wear damage was achieved by feeding the amplitudes of the harmonics of the tooth mesh frequency from both the vibration and acoustic signal into a multilayer perceptron artificial neural network. In the study conducted by Hsiao, Shivam and Kam (2020), vibration signals from a three-axis vibration sensor were input into an ensemble of a convolutional neural network for automatic feature extraction and a fully convolutional network for damage detection. This ensemble achieved a damage detection accuracy of 97 %.

2.2.3. Classification of Multiple Damages in Worm Gears

In three studies, the authors Karabacak, Gürsel and Gümüşel (2020), Karabacak et al. (2022) and Karabacak et al. (2022), investigated the classification of different damage types in worm gears, including artificial wear, pitting and tooth fracture. In one study, the researchers compared the suitability of thermal images and the short-time Fourier transformation spectrograms of vibration and acoustic signals for damage classification. As demonstrated in the study, the trained convolutional neural networks achieved a classification rate of 100 % using thermal images, 83.3 % using vibration signals, and 81.7 % using acoustic signals. In a subsequent study Karabacak et al. (2022) employed a common spatial pattern for feature extraction from vibration and acoustic signals. Among the downstream methods considered for damage classification, an artificial neural network achieved the best results with a classification rate of 88.9 % for vibration signals and 99.1 % for acoustic signals. To further improve classification performance, the authors combined features from thermal images, vibration signals

and acoustic signals. Using this approach, the artificial neural network achieved a damage detection rate of 99.2 % and a damage classification rate of 98.6 %. When the same features were incorporated into a support vector machine, the damage detection and classification rate were 98.7 % and 98.9 %.

2.3. Research Gap

The aforementioned studies focused on the detection of damage on the worm wheel, namely pitting, wear and tooth fracture. However, the existing literature has not yet addressed damage occurring on the worm. One such type of damage is breakout damage, which is occasionally observed on the tooth flank of case-hardened steel worms. It is presumed to occur at the beginning of worm gear operation, when the contact pattern is not yet fully developed and local contact pressures are high. Damage to the worm leads to accelerated abrasive wear on the softer worm wheel material. Consequently, this type of damage is also highly relevant for condition monitoring, similar to conventional wear on the worm wheel. The objective of this study is to detect and classify these two types of damage, namely breakout on the worm and wear on the worm wheel. This enables the implementation of damage-specific measures within a PHM framework.

3. MATERIALS AND METHODS

To achieve this objective of the study, vibration data obtained from a worm gear test bench is evaluated. Measurements are conducted under different operating conditions and for different types of artificial worm gear damage. The vibration data is evaluated in the frequency domain by comparing the vibration amplitudes at characteristic frequencies between damaged and undamaged worm gear conditions. The experimental setup, test series and vibration data evaluation procedure are described in detail in the following.

3.1. Experimental Setup

All experimental investigations are conducted on the test bench depicted in Figure 1.

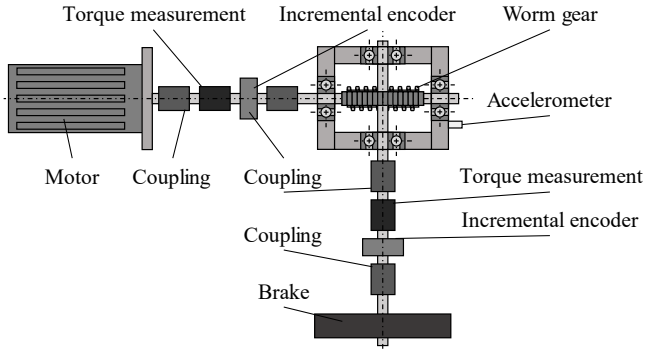

Figure 1. Worm gear test bench.

The worm gear under investigation is driven by an electric motor. Torque measurement shafts and incremental encoders are integrated into the power flow before and after the worm gear. Torque is applied to the worm gear using a magnetic particle brake. The tested worms are case-hardened steel worms with a module of 1.75 mm. The worm wheel is made of brass and contains 44 teeth. An accelerometer is mounted close to the bearing of the worm for damage detection. The measurement direction is parallel to the axis of the worm. The vibration data is sampled at a frequency of 40 kHz. In the subsequent sections, the artificially manufactured damages as well as the corresponding test plans used for their investigation are described. As outlined in the research gap, two distinct types of damage are examined in this study: pitting-like breakouts on the worm and wear on the worm wheel. In real operating conditions, these damage types may be interdependent and can occur consecutively. However, since wear damage on the worm wheel can also occur independently, both damage types are analyzed in two series of experimental investigations.

3.2. Experimental Investigations on Breakouts on the Worm

For the investigation on breakout damage on the worm, the tested parameters and parameter levels are summarized in Table 1. Given the lack of literature on this damage type, the present study aims for an initial investigation on damage detection under different operating conditions in terms of rotational speed and torque. For this purpose, a reduced-scale test plan featuring no replications is employed. The parameter levels from Table 1 are combined in a full factorial design of experiments (DOE) test plan. The rotational speed is set by the motor and therefore refers to the input side of the worm gear. The torque is applied by the magnetic particle brake. Consequently, the torque levels listed in Table 1 refer to the output side of the worm gear.

Table 1. Tested parameters and levels for breakout damage on the worm.

Parameter	Levels		
Rotational speed [min^{-1}]	361	1,440	2,859
Torque [Nm]	37	130	
Damage	None	Small	Large

Two worm specimens are initially measured at the illustrated levels of rotational speed and torque in an undamaged state. Then artificial damage of different size is manufactured on each worm using a milling machine, and the measurements at different levels of rotational speed and torque are conducted again. The large state of the artificial breakout damage to the tooth flank of the worm is depicted in Figure 2. The damage is produced twice on the tooth flank of the worm.

Figure 2. Artificial breakout damage on the worm.

The measurement data from the test bench is recorded for 100 seconds in stationary operating conditions resulting from the DOE test plan.

3.3. Experimental Investigations on Wear on the Worm Wheel

To extend the existing literature on wear damage on the worm wheel, a more extensive test plan is developed to investigate the influence of rotational speed and torque on the detectability of the damage. The parameters and their respective levels are summarized in Table 2. As in Table 1, the rotational speed refers to the input side of the worm gear, while the torque values refer to the output side. Wear damage on the worm wheel affects both tooth flanks. Consequently, both directions of rotation are considered in this experimental series and are indicated by the sign of the rotational speed.

Table 2. Tested parameters and levels for wear damage on the worm wheel.

Parameter	Levels		
Rotational speed [min^{-1}]	± 1,315	± 2,620	± 3,483
Torque [Nm]	31	78	120
Damage	None	Small	Large

The six levels of rotational speed, three levels of torque, three damage levels, and one replication of the test plan are combined in a full factorial design comprising 108 experiments. For each stage of damage, the order of testing for different rotational speeds and torque levels is randomized. The different stages of artificial wear damage are produced on different worm wheels. The replication of the experiments is conducted to account for variations in the vibration signal caused by replacing the worm wheel with a specimen representing a different damage stage. The different stages of artificial wear damage on the worm wheel are depicted in Figure 3.

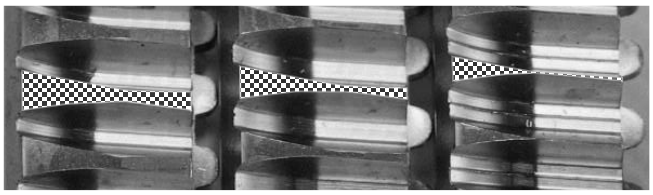

Figure 3. Artificial wear damage on three worm wheels.

The top land area of one tooth is highlighted to illustrate the effect of the artificial wear damage as a reduction of the tooth thickness. In this experimental series, the sensor data is recorded for 25 revolutions of the worm wheel for each stationary operating condition resulting from Table 2.

3.4. Evaluation of the Vibration Data

The vibration data from the accelerometer is evaluated in the frequency domain for damage detection. The transformation into the frequency domain is performed by using the fast Fourier transform (FFT).

3.4.1. Data Evaluation for Detection of the Breakout Damage on the Worm

The artificial breakout damage on the worm meshes with the worm wheel at least once per revolution. As the damage is produced multiple times on the worm tooth, a damage-related influence on the vibration signal is expected at multiples of the rotational frequency of the worm. In gear diagnostics, the vibration at the gear mesh frequency (GMF) is commonly used to identify tooth damage. The GMF is defined as the product of the gear rotational frequency and the number of gear teeth. Due to the worm's singular tooth, the rotational frequency corresponds to the GMF. An excerpt of the frequency spectrum of the vibration data from a measurement with breakout damage on the worm is shown in Figure 4. The harmonics of the GMF are indicated by dashed lines.

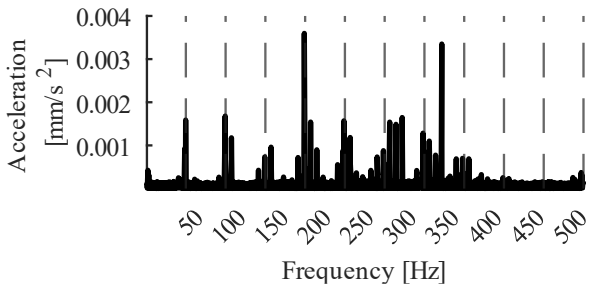

Figure 4. Frequency domain of vibration data with breakout damage on worm, marked harmonics of the GMF.

The amplitudes at the harmonics of the GMF are found to vary depending on the operating conditions. At lower rotational speeds, the harmonics of the GMF appear less distinct and merge more closely with the noise of the measured vibration signal. As illustrated in Figure 4, the amplitudes at the harmonics of the GMF decrease with increasing harmonic order. It is determined that, for all

operating conditions, the first ten harmonics of the GMF can be evaluated before the amplitudes become indistinguishable from the noise level of the vibration signal. The change in the amplitudes of those harmonics of the GMF is then calculated from the measurement obtained with artificial breakout damage to the measurement obtained under identical operating conditions without damage. By calculating the changes, the discrepancies between the amplitudes of the frequency spectra with and without damage are not weighted by the magnitude of the amplitudes. The calculated changes for each harmonic of the GMF are then consolidated into a single value using the geometric mean. This value represents an overall trend of the damage effect on the vibration amplitudes at the analyzed frequencies. A sensitivity analysis is performed to determine an appropriate number of harmonics that is robust against outliers while still sufficiently representing the effect of the damage.

3.4.2. Data Evaluation for Detection of the Wear Damage on the Worm Wheel

Both artificial and natural wear damage on the worm wheel affect all teeth. Consequently, no periodic effect in the vibration signal is anticipated. As shown in the frequency spectra in Figure 5, there is a notable increase in vibration amplitudes around 8 kHz when wear damage is present on the worm wheel. This observation is consistent across all 108 conducted measurements.

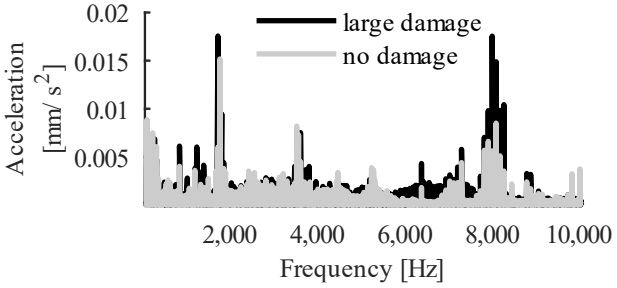

Figure 5. Frequency domain of vibration data with and without wear damage on worm wheel.

Based on this observation, the mean value of all amplitudes within the frequency band between 7.5 kHz and 8.5 kHz is calculated for damage detection and for the evaluation of the DOE test plan. Since this frequency band does not vary with different levels of rotational speed, it is likely a natural frequency of a component of the gearbox, which is stimulated by the damage.

4. RESULTS

The results obtained from the separate experimental series are presented in the following sections.

4.1. Detection of Breakout Damage on the Worm

The calculated damage detection values for the corresponding operating conditions are shown Figure 6. Based on the sensitivity analysis, the changes in amplitude at the first four harmonics of the GMF are consolidated into a damage detection value, as this configuration proves the highest damage detectability. Due to the limited number of measurements, a statistical evaluation of the experiments is not meaningful.

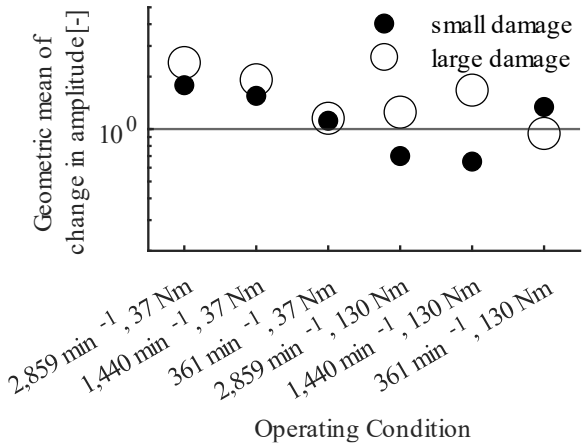

Figure 6. Calculated values for damage detection of breakout damage on worm.

In Figure 6 the horizontal line at a value of one indicates a state in which no change in amplitude at the examined GMF harmonics is caused by the damage. As shown in Figure 6, a consistent trend of average changes greater than one can be observed for the lower torque level. In this case, the vibration amplitudes at the first four harmonics of the GMF are, on average, higher when breakout damage is present on the worm. For the higher torque level, the calculated values lie both below and above the value of one, which does not indicate a consistent trend. Furthermore, the calculated values fail to reflect the size of the breakout damage.

4.2. Detection of Wear Damage on the Worm Wheel

For the damage detection according to the DOE test plan, the mean value of the vibration amplitudes within the frequency band between 7.5 kHz and 8.5 kHz is used as the target value. An analysis of variance (ANOVA) is subsequently conducted to identify the influence of the examined parameters on this target value. The resulting model describing the target value features an adjusted R-Squared value of 84.8 %. At a significance level of 5 %, the significant parameters include the main effects of damage, rotational speed, and torque, as well as the interaction between damage and replication. The main effects of the model, including the corresponding 95 % confidence intervals are presented in Figure 7.

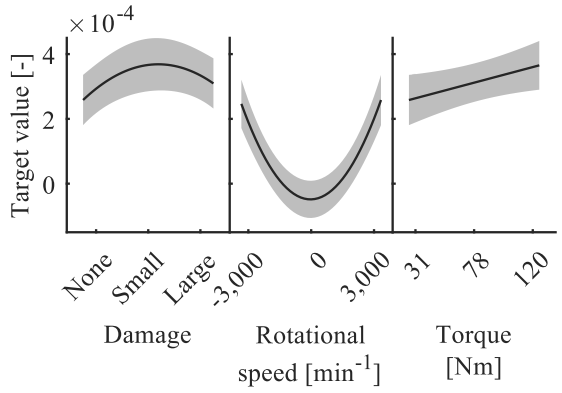

Figure 7. Main effects diagram of ANOVA results.

As illustrated in the main effects diagram, rotational speed exerts the strongest effect on the target value. The magnitude of the target value increases with an increasing rotational speed. Based on the parabolic main effect, it can be concluded that the effect of rotational speed is consistent for both directions of rotation. For torque, a linear increase in the target value is observed with increasing torque. The size of the damage also affects the vibration amplitudes within the frequency band between 7.5 kHz and 8.5 kHz. Interestingly, the small damage state leads to a larger increase in amplitudes than the large damage state. Furthermore, the interaction between the damage and the replication significantly influences the target value. This effect may be attributed to the remounting of the worm wheel with a specific artificial damage for each execution of the experiments, which also affects the vibration paths.

5. DISCUSSION

The results indicate that breakout damage on the worm may be detectable in the amplitudes at the harmonics of the GMF. For the low torque level, the first four harmonics of the GMF show, on average, higher amplitudes in the measurements of the damaged state compared to the undamaged state. At the high torque level, the observed vibration behavior may be influenced by the fact that the applied torque exceeds the nominal value for this worm gear size, as specified in the 2020 International Organization for Standardization report. One possible explanation is elastic deformation of the teeth during meshing, which may affect the tooth meshing behavior and, consequently, the frequencies and amplitudes of the vibration signal. This effect may complicate the separation of damage-related features from load-dependent effects, which is why there is no consistent trend in Figure 6 for the high level of torque. However, due to the limited number of experiments and the absence of replications, these findings should be considered preliminary. Additional experiments are required to validate the observed trends and to quantify the influence of variability sources, such as operating conditions. Only then can the appropriate number of GMF harmonics for robust damage detection be determined.

The detection of wear damage on the worm wheel appears to be more robust than the detection of breakout damage on the worm, as reliable discrimination was achieved across all tested speed and torque levels. However, these results should still be interpreted with caution, since only one replication of the test plan was performed. Additional replications are required to obtain a more reliable statistical assessment of variability effects. A significant effect on the target value was observed for the interaction between execution and damage. This effect is suspected to be caused by the remounting of the tested gearbox for the testing of worm wheels of different damage states. Since a worm gearbox is typically not remounted during normal operation, this effect is of limited relevance for practical condition monitoring. The main effect of damage shown in Figure 7 indicates that small damage has a greater influence on the target value than large damage. In the context of condition monitoring, however, this effect is of secondary importance, since naturally occurring damage progresses from small to severe damage and can therefore be detected at an early stage. This early damage detectability enables the application of PHM measures following damage detection. It should also be noted that the frequencies used for damage detection in this study may be specific to the investigated gearbox. Since these evaluated frequencies are the same for all rotational speeds, they likely correspond to natural frequencies of gearbox components that are excited by rotational speed, torque, and damage. Although the proposed evaluation method proved effective for the tested gearbox, further research is required to assess the transferability of the identified frequency features to other gearbox designs.

Finally, all experimental investigations were conducted using artificial damage on the worm and worm wheel. While this approach enables controlled and reproducible testing conditions, the transferability of the proposed methods to naturally occurring damage remains to be verified.

6. CONCLUSIONS

In this study, the distinction of a damaged worm gear from an undamaged worm gear has been achieved for two relevant types of damage in the context of maintenance strategies. For the breakout damage on the tooth flank of a case-hardened worm, a consistent trend compared with measurements obtained from undamaged specimens was observed in the vibration data at low torque levels. Wear damage on the worm wheel can be detected in the investigated worm gearbox for all tested operating conditions of rotational speed and torque. The classification of damage types is possible due to the use of different methods of vibration data evaluation. This result enables the implementation of damage-specific maintenance strategies.

REFERENCES

Daubach, K., Oehler, M. & Sauer, B. (2022). Wear simulation of worm gears based on an energetic approach. *Forschung im Ingenieurwesen*, vol. 86 (3), pp. 367-377. doi:10.1007/s10010-021-00525-3

Elasha, F., Ruiz-Cárcel, C., Mba, D., Kiat, G., Nze, I. & Yebra, G. (2014). Pitting detection in worm gearboxes with vibration analysis. *Engineering Failure Analysis*, vol. 42, pp. 366-376. doi:10.1016/j.engfailanal. 2014.04.028

Hammami, C., Chakroun, A. E., Chaari, F., Hammami, A., De-Juan, A., Fernandez, A., Viadero, F. & Haddar, M. (2022). Estimation of Vibrations Levels of a Worm Gear Model with Plastic Wheel. *Design and Modeling of Mechanical Systems - V*, pp. 646–654. doi:10.1007/978-3-031-14615-2_72

Hizarci, B., Ümütlü, R. C., Kıral, Z. & Öztürk, H. (2021). Fault severity detection of a worm gearbox based on several feature extraction methods through a developed condition monitoring system. *SN Applied Sciences*, vol. 3 (1). doi:10.1007/s42452-020-04131-w

Hsiao, J. C., Shivam, K., & Kam, T. Y. (2020). Fault diagnosis method for worm gearbox using convolutional network and ensemble learning. *Journal of Physics: Conference Series*, vol. 1509 (1). doi:10.1088/1742-6596/1509/1/012030

International Standards Organization (ISO) (2020). Gears - Calculation of load capacity of worm gears. In ISO, *ISO/TS14521:2020* (ISO). Genève, Switzerland: International Standards Organization.

Jbily, D., Guingand, M. & Vaujany, J. (2016). A wear model for worm gear. *Proceedings of the Institution of Mechanical Engineers, Part C: Journal of Mechanical Engineering Science*, vol. 230 (7-8), pp. 1290-1308. doi:10.1177/0954406215606747

Karabacak, Y., Gürsel Ö. N. & Gümüşel, L. (2020). Worm gear condition monitoring and fault detection from thermal images via deep learning method. *Eksploatacja i Niezawodność – Maintenance and Reliability*, vol. 22 (3), pp. 544-556. doi:10.17531/ein.2020.3.18

Karabacak, Y., Gürsel Ö. N. & Gümüşel, L. (2022). Common spatial pattern-based feature extraction and worm gear fault detection through vibration and acoustic measurements. *Measurement*, vol. 187. doi:10.1016/j.measurement.2021.110366

Karabacak, Y., Gürsel Ö. N. & Gümüşel, L. (2022). Intelligent worm gearbox fault diagnosis under various working conditions using vibration, sound and thermal features. *Applied Acoustics*, vol. 186. doi:10.1016/ j.apacoust.2021.108463

Opalić, M., Žeželj, D. & Vučković, K. (2015). A new method for description of the pitting process on worm wheels propagation. *Wear*, vol. 332-333, pp. 1145-1150. doi:10.1016/j.wear.2015.01.053

Peng, Z. & Kessissoglou, N. (2003). An integrated approach to fault diagnosis of machinery using wear debris and vibration analysis. *Wear*, vol. 255 (7-12), pp. 1221-1232. doi:10.1016/S0043-1648(03)00098-X

Raadnui, S. (2021). Condition monitoring of worm gear wear and wear particle analysis of industrial worm gear sets. *Wear*, vol. 476. doi:10.1016/j.wear.2021.203687

Randall, R. B., (2011). *Vibration-based Condition Monitoring*. Chichester: Wiley.

Sharif, K. J., Evans, H. P. & Snidle, R. W. (2006). Prediction of the wear pattern in worm gears. *Wear*, vol. 261 (5-6), pp. 666-673. doi:10.1016/j.wear.2006.01.018

Schnetzer, P. E., Pellkofer, J. & Stahl, K. (2023). Calculation method for wear of steel-bronze rolling-sliding contacts relating to worm gears. *Forschung im Ingenieurwesen*, vol. 87 (3), pp. 961-971. doi:10.1007/s10010-023-00692-5

Tao, Z., Chen, H., Zhang, X. & Jiang, Y. (2021). Failure analysis of worm gear in worm transmission. *Journal of Physics: Conference Series*, vol. 1965 (1). doi:10.1088/1742-6596/1965/1/012132

Ümütlü, R. C., Hizarci, B., Öztürk, H. & Kiral, Z. (2016). Pitting detection in a worm gearbox using artificial neural networks. *InterNoise16*, pp. 6526-6534.

Ümütlü, R. C., Hizarci, B., Ozturk, H. & Kiral, Z. (2020). Classification of pitting fault levels in a worm gearbox using vibration visualization and ANN. *Sādhanā*, vol. 45 (22). doi:10.1007/s12046-019-1263-1

Vojtko, I., Kočiško, M., Šmeringaiová, A. & Adamčík, P. (2013). Vibration of worm gear boxes. *Applied Mechanics and Materials*, vol. 308, pp. 45-49. doi:10.4028/www.scientific.net/AMM.308.45

Waqar, T. & Demetgul, M. (2016). Thermal analysis MLP neural network based fault diagnosis on worm gears. *Measurement*, vol. 86, pp. 56-66. doi:10.1016/ j.measurement. 2016.02.024

Ya-xiong, Z., Ke-jian, M., Yan, L., Lin, Q., Zhan-xiu, L. & Wei-min, Z. (1988). An analysis of the wear features of worm gear tooth flanks. *Tribology International*, vol. 21 (5), pp. 281-285. doi:10.1016/0301-679X(88)90006-0